

CHARACTERIZATION OF CHEMICALLY VAPOR INFILTRATED SILICON CARBIDE COMPOSITES REINFORCED BY VARIOUS HIGH MODULUS FIBERS: II. TENSILE PROPERTIES

—T. Nozawa, Y. Kato, L. L. Snead (Oak Ridge National Laboratory), T. Hinoki and A. Kohyama (Kyoto University, Japan)

OBJECTIVE

The objective in this study is to evaluate the fundamental mechanical properties of various architecture types of SiC/SiC and hybrid SiC-C/SiC composites reinforced by high-modulus SiC and carbon fibers, designed to provide high thermal conductivity.

SUMMARY

Tensile properties of SiC/SiC composites were significantly dependent on the axial fiber volume fraction; three-dimensional (3D) SiC/SiC composites with in-plane fiber content <15% exhibited lower tensile strength and proportional limit stress. The composites with high volume fraction of the axial fibers >20% exhibited improved tensile properties. In contrast, the hybrid SiC-C/SiC composites with severe matrix damage induced by the large mismatch of coefficients of thermal expansion between the fiber and the matrix exhibited low tensile tangent modulus and proportional limit stress.

PROGRESS AND STATUS

Introduction

Advanced SiC/SiC composites with the highly-crystalline SiC fibers and the matrix are beneficial to improve system efficiency and allow higher resistance to thermal shock because of their enhanced thermal and thermo-mechanical properties. In Part I [1], it was revealed that the 3D Tyranno™-SA fiber composites showed the excellent thermal transport properties (~55 W/m-K) due to excellent thermal conductivity of Tyranno™-SA, ~65 W/m-K. In contrast, the hybrid SiC-C/SiC composites incorporated with the carbon fibers were prevented heat transport via matrix due to severe damage in the matrix by the large mismatch of coefficients of thermal expansion between the carbon fiber and the SiC matrix.

The latest composites with the high modulus SiC fibers, i.e., highly-crystalline and near-stoichiometric SiC fibers: Tyranno™-SA and Hi-Nicalon™ Type-S, and the β -SiC matrix provide good geometrical stability and strength retention after neutron irradiation [2–4]. However, mechanical property data of the advanced SiC/SiC composites are still insufficient and strongly required to obtain for practical applications.

Experimental Procedure

A plain-weave Tyranno™-SA/CVI-SiC (P/W SA), a satin-weave Hi-Nicalon™ Type-S/SiC (S/W HNLS), and two types of 3D Tyranno™-SA/CVI-SiC composites with the fabric configurations of X:Y:Z=1:1:4 and 1:1:1 (3D(1:1:4) SA and 3D(1:1:1) SA) were prepared. In addition, P/W and 3D hybrid SiC-C/SiC composites incorporated with the P120S carbon fibers (Hybrid 2D and Hybrid 3D) were fabricated to give improved thermal conductivity. All composites had 150 nm-thick pyrolytic carbon as fiber/matrix interphase. Details of materials were summarized in Table 1 of Part I [1].

Tensile specimens were machined from the composite plates so that the longitudinal direction was parallel to either of X or Y fiber directions. Miniature tensile geometry that had been developed for neutron irradiation studies on ceramic composites [5] was employed. The rectangular geometry (length × width × thickness) of 15.0 mm × 4.0 mm × 2.3 mm was used, except for the 3D SiC/SiC composites with 20.0 mm × 6.0 mm × 2.5 mm. Tensile tests were conducted following the general guidelines of ASTM standard C1275. For the testing at room temperature, specimens were clamped by wedge grips with aluminum end tabs on both faces of the gripping sections. The strain was determined by averaging the readings of strain gauges bonded to both faces of the center gauge section. The crosshead displacement rate was 0.5 mm/min for all tests.

Results and Discussion

Figure 1 exhibits the typical tensile stress-strain curves and tensile data are listed in Table 1. Each of the curves for 2D SiC/SiC composites comprises an initial proportional segment that corresponds to the elastic deformation, followed by a second linear portion during which matrix cracks in transverse fiber bundles progressively develop, and a further non-linear portion due to domination of the matrix cracks in the longitudinal fiber bundles and the fiber failures. The tensile strength of 200~300 MPa for 2D SiC/SiC composites is similar to that obtained from conventional 2D CVI-SiC/SiC composites [6]. The higher tensile tangent modulus of ~270 GPa of the 2D SiC/SiC composites is attributed to the use of the highly-crystalline SiC fibers and the β -SiC matrix. The large scatters were due to varied pore content. The 3D SiC/SiC composites exhibited high elastic modulus, though significantly lower tensile strength than the 2D CVI SiC/SiC composites. They are roughly distinguished into two types of fracture patterns: brittle and quasi-ductile with non-linear portion beyond initial linear segment, although both fracture behaviors exhibited limited short fiber pullout. Most of the brittle specimens failed after the first proportional limit stress, resulting in lower tensile strength, ~65 MPa.

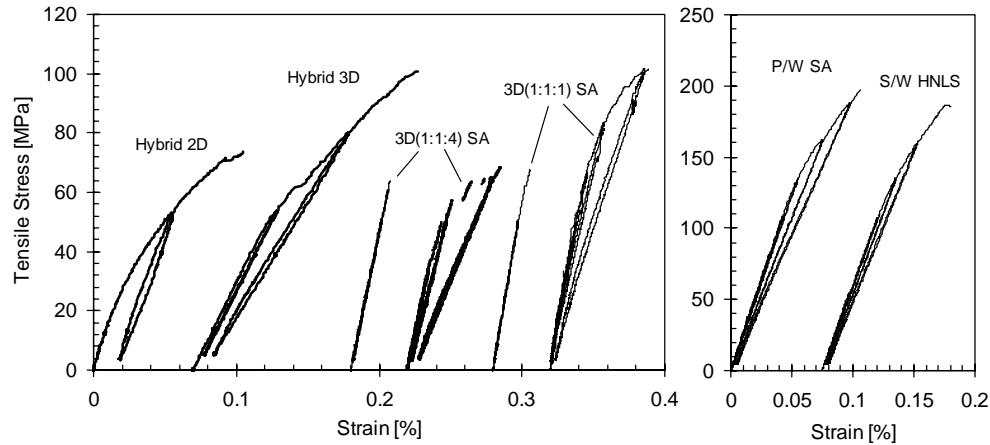


Fig. 1. Typical tensile stress-strain curves of various CVI SiC/SiC and hybrid SiC-C/SiC composites.

Table 1. Reduced tensile data of various SiC/SiC and hybrid SiC-C/SiC composites

Composite ID	Tensile tangent modulus [GPa]	First proportional limit stress [MPa]	Second proportional limit stress [MPa]	Ultimate tensile strength [MPa]	Misfit stress [MPa]
P/W SA	273(23)	103(21)	135(15)	199(2)	24(9)
S/W HNLS	244(6)	101(9)	145(4)	226(50)	15(4)
3D(1:1:4) SA - brittle	213(26)	64	-	64	-
3D(1:1:4) SA	224(5)	35(2)	49(1)	59(13)	4(2)
3D(1:1:1) SA - brittle	264(18)	60(4)	-	65(4)	-
3D(1:1:1) SA	277	53	70	102	2(4)
Hybrid 2D	138(28)	8(1)	23(3)	94(28)	32
Hybrid 3D	95(10)	47(1)	82(14)	98(3)	18(4)

*The numbers in parenthesis indicate standard deviation.

A feature of the hybrid composites is significantly lower elastic moduli, ~140 GPa for 2D and ~100 GPa for 3D, respectively. In contrast, the estimated elastic moduli by parallel-serial approach based on the rule of mixtures [7] yielded ~270 GPa for 2D and ~100 GPa for 3D. It is noted that the elastic modulus of P/W hybrid composites was roughly estimated by replacing with the orthogonal 2D architecture. Therefore the estimated elastic modulus should be influenced by pore distribution and waviness. Processing-induced matrix cracks perpendicular to the loading axis of the 2D hybrid composites severely reduced initial tensile tangent modulus. Damaged matrices also caused less proportional segment, followed by progressive damage accumulations in lower stress level. Contrarily, the 3D hybrid composites with transverse matrix

cracks around Z-stitch carbon fibers, which existed parallel to the axial fibers, exhibited less degradation of the elastic modulus.

The significant difference of tensile strength in the composite types is attributed primarily to the effective fiber volume content in the loading axis. According to Curtin [8], the intact fibers transfer the applied load beyond the fiber failure. In particular, it is simply assumed that intact fibers equally convey the applied load, well known as the global load sharing (GLS) theory. This indicates that the ultimate tensile strength is proportional to the axial fiber volume fraction. Composites tested in this study were designed with varied fiber volume content. As plotted in Fig. 2(a), the large differences in axial fiber content provided the differed tensile strength in each composite. Both 3D SiC/SiC composites with large structural unit, ~ 3.0 mm, are subjected to change in fiber volume fraction in cutting position. The bare fibers located at the edges of the specimen are mostly damaged, i.e., discontinuous along the gauge length, and those are ineffective in load transfer. In this case, less ability to transfer the applied load resulted in the quasi-brittle failure at the first proportional limit stress. In addition, the possible slight processing damage on reinforcing fibers of 3D SiC/SiC composites during heating up to 2073 K may have degraded the tensile strength.

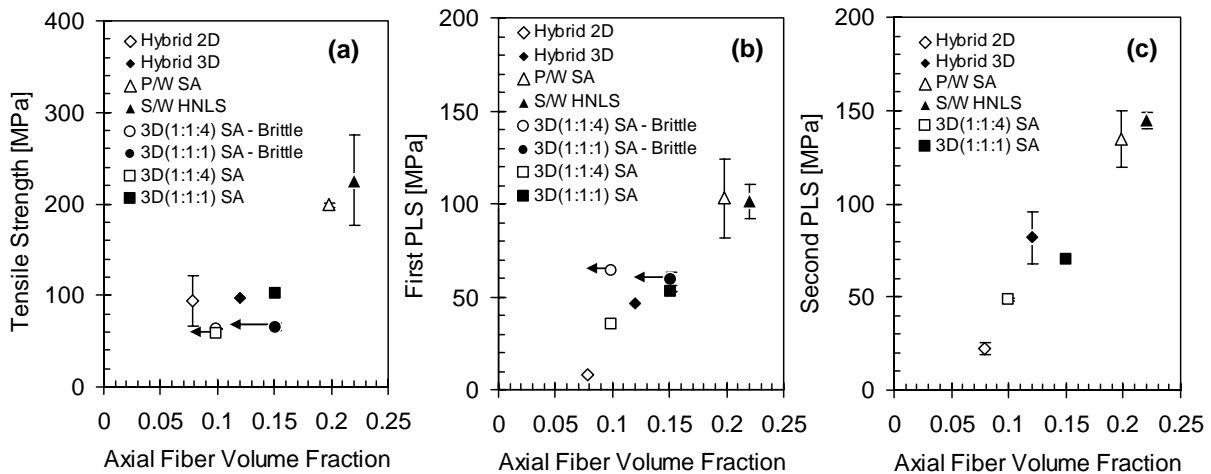


Fig. 2. Relationships among tensile properties and the axial fiber volume fraction.

As with the tensile strength, the difference of the proportional limit stress (PLS) in composite types may be attributed primarily to the axial fiber volume content (Figs. 2(b) and (c)). In particular, the 2D hybrid composites with severe processing-induced matrix damages had lower PLS, although, in many cases, it is very difficult to define the second PLS from the stress-strain curve because of progressive damage

accumulation. Degradation of the reloading modulus at the lower stress level supports progressive damage accumulation.

The residual thermal stress is inevitable when the coefficients of thermal expansion are different between the fibers and the matrix. In the Tyranno™-SA or Hi-Nicalon™ Type-S/PyC/CVI-SiC system, the residual stress should be minimal, because the fibers consist primarily of cubic (beta-phase) SiC, i.e., equivalent to the matrix constituent. The thermal residual stress estimated by the method proposed by Vagaggini et al. [9] exhibits nearly zero for 3D SiC/SiC composites and residual tension of ~20 MPa for 2D SiC/SiC composites (Table 1). The slightly larger residual stress of 2D SiC/SiC composites might be due to restriction by waviness. The hybrid SiC-C/SiC composites exhibited relatively higher tensile residual stress due to large CTE mismatch of the SiC and the carbon.

Acknowledgements

The authors would like to thank Dr. Edgar Lara-Curzio at Oak Ridge National Laboratory for mechanical testing. This research was sponsored by the Office of Fusion Energy Sciences, U.S. Department of Energy under contract DE-AC05-00OR22725 with UT-Battelle, LLC, and 'JUPITER-II' U.S. Department of Energy/Japanese Ministry of Education, Culture, Sports, Science and Technology (MEXT) collaboration for fusion material system research.

References

- [1] T. Nozawa, Y. Katoh, L. L. Snead, T. Hinoki, and A. Kohyama, submitted to Fusion Materials Semiannual Progress Report for Period Ending December 31, 2004, DOE/ER-0313/37, U.S. Department of Energy.
- [2] L. L. Snead, Y. Katoh, A. Kohyama, J. L. Bailey, N. L. Vaughn, and R. A. Lowden, *J. Nucl. Mater.* 283–287 (2000) 551.
- [3] T. Hinoki, L. L. Snead, Y. Katoh, A. Hasegawa, T. Nozawa, and A. Kohyama, *J. Nucl. Mater.* 307–311 (2002) 1157.
- [4] T. Nozawa, L. L. Snead, Y. Katoh, and A. Kohyama, *J. Nucl. Mater.* 329–333 (2004) 544.
- [5] T. Nozawa, Y. Katoh, A. Kohyama, and E. Lara-Curzio, *Proceedings of the Fifth IEA Workshop on SiC/SiC Composites for Fusion Energy Application*, International Energy Agency, 74 (2002).
- [6] Y. Katoh, A. Kohyama, T. Hinoki, and L. L. Snead, *Fus. Sci. Technol.* 44 (2003) 155.
- [7] T. Ishikawa, K. Bansaku, N. Watanabe, Y. Nomura, M. Shibuya, and T. Hirokawa, *Compos. Sci. Technol.* 58 (1998) 51.

[8] W. A. Curtin, *J. Am. Ceram. Soc.* 74 (1991) 2837.

[9] E. Vagaggini, J-M. Domergue, and A. G. Evans, *J. Am. Ceram. Soc.* 78 (1995) 2709.